

# Climate Dynamics

## HighResMIP models improves detection of intense cyclones over southeast South America

--Manuscript Draft--

Manuscript Number:		
Full Title:	HighResMIP models improves detection of intense cyclones over southeast South America	
Article Type:	Original Article	
Keywords:	HighResMIP; Intense extratropical cyclones; High-resolution models; Southeast South America.	
Corresponding Author:	Henri Pinheiro University of Sao Paulo: Universidade de Sao Paulo Sao Jose dos Campos, SP BRAZIL	
Corresponding Author Secondary Information:		
Corresponding Author's Institution:	University of Sao Paulo: Universidade de Sao Paulo	
Corresponding Author's Secondary Institution:		
First Author:	Henri Pinheiro	
First Author Secondary Information:		
Order of Authors:	Henri Pinheiro Tercio Ambrizzi	
Order of Authors Secondary Information:		
Funding Information:	Conselho Nacional de Desenvolvimento Científico e Tecnológico (151225/2023-0) Fundação de Amparo à Pesquisa do Estado de São Paulo (2023/10882-2)	Dr Henri Pinheiro Dr Henri Pinheiro
Abstract:	<p>Extratropical cyclones play a critical role in midlatitude climate dynamics, but their accurate simulation remains a challenge in climate models. While enhanced resolution simulations have been widely used to study these systems in the Northern Hemisphere, their performance in the Southern Hemisphere, particularly for intense cyclones, remains less explored. This study evaluates the impact of increased horizontal resolution on the simulation of extratropical cyclones over a key hotspot in southeastern South America, comparing HighResMIP models (25–50 km) with standard CMIP6 models (100–250 km). Using an objective feature-tracking algorithm applied to T42 vorticity at 850 hPa, we analyze cyclone frequency, intensity, structure, and life cycle, comparing against ERA5 reanalysis. Results show that finer resolution models reduce biases in cyclone number and track density, significantly improving the detection of intense cyclones, whereas coarser resolution models underestimate their frequency by more than 50%. The higher resolution models also better capture peak cyclone intensity, while their lower resolution counterparts fail to identify extreme events. Additionally, increased resolution enhanced the representation of cyclone structure and evolution, particularly in terms of maximum vorticity and wind speed. However, both model groups struggle to simulate precipitation patterns, underscoring persistent challenges in cyclone-related convection processes. These findings highlight the advantages of higher resolution models in representing extreme cyclones and provide a foundation for improved climate projections under future warming scenarios.</p>	
Suggested Reviewers:	Jennifer Catto jlcatto@exeter.ac.uk Expertise in extratropical cyclones, extreme weather, and resolution-dependent model performance. Active in CMIP6/HighResMIP analysis, particularly for precipitation	

	processes.
	<p>Christian Seiler  christian.seiler@queensu.ca  has published on extratropical cyclones in climate models, including evaluation of explosive cyclones in CMIP5/6.</p>
	<p>Victoria Sinclair  victoria.sinclair@helsinki.fi  She is an expert in extratropical cyclone dynamics and has published on cyclone structure, climatology, and future projections using both reanalyses and climate model data.</p>
	<p>Noboru Nakamura  nnn@uchicago.edu  Authority on midlatitude dynamics, vorticity-based cyclone diagnostics, and model resolution impacts.</p>

Dear Editor,

I am pleased to submit our manuscript titled "HighResMIP Models Improve Detection of Intense Cyclones over Southeast South America" for consideration for publication in Climate Dynamics. This study evaluates the performance of HighResMIP models in detecting intense cyclones in the region of southeast South America, contributing to the broader understanding of cyclone dynamics and the application of high-resolution climate models in extreme weather events. We believe this work aligns well with the journal's focus on numerical modeling and climate dynamics.

Thank you for considering our submission. We look forward to your feedback and the opportunity to contribute to the journal.

Best regards,

Henri Pinheiro

# HighResMIP models improves detection of intense cyclones over southeast South America

Henri Pinheiro<sup>1</sup> and Tercio Ambrizzi<sup>1</sup>

<sup>1</sup>Department of Atmospheric Sciences, University of Sao Paulo, 05508-090, Brazil.

*Correspondence to:* Henri Pinheiro ([henri.pinheiro@usp.br](mailto:henri.pinheiro@usp.br))

<https://orcid.org/0000-0003-4363-3206>

## Abstract

Extratropical cyclones play a critical role in midlatitude climate dynamics, but their accurate simulation remains a challenge in climate models. While enhanced resolution simulations have been widely used to study these systems in the Northern Hemisphere, their performance in the Southern Hemisphere, particularly for intense cyclones, remains less explored. This study evaluates the impact of increased horizontal resolution on the simulation of extratropical cyclones over a key hotspot in southeastern South America, comparing HighResMIP models (25–50 km) with standard CMIP6 models (100–250 km). Using an objective feature-tracking algorithm applied to T42 vorticity at 850 hPa, we analyze cyclone frequency, intensity, structure, and life cycle, comparing against ERA5 reanalysis. Results show that finer resolution models reduce biases in cyclone number and track density, significantly improving the detection of intense cyclones, whereas coarser resolution models underestimate their frequency by more than 50%. The higher resolution models also better capture peak cyclone intensity, while their lower resolution counterparts fail to identify extreme events. Additionally, increased resolution enhanced the representation of cyclone structure and evolution, particularly in terms of maximum vorticity and wind speed. However, both model groups struggle to simulate precipitation patterns, underscoring persistent challenges in cyclone-related convection processes. These findings highlight the advantages of higher resolution models in representing extreme cyclones and provide a foundation for improved climate projections under future warming scenarios.

**Keywords:** HighResMIP; Intense extratropical cyclones; High-resolution models; Southeast South America.

## 1 Introduction

Extratropical cyclones are a dominant feature of the midlatitude climate, playing a critical role in the global circulation by transporting heat, moisture, and momentum. These systems are also responsible for extreme precipitation and strong winds, which can have significant socioeconomic impacts, particularly in regions as southeast South America (Bitencourt et al. 2010, Gobato and Heidari 2020). Understanding extratropical cyclone characteristics under present-day climate conditions is essential for improving future climate projections and risk assessments. However, accurately simulating these systems, especially their associated extreme impacts, remains a challenge in climate models (Catto et al. 2010; Priestley et al. 2020). A key factor influencing their representation is horizontal resolution, which affects the model’s ability to capture small-scale processes critical to cyclone development and evolution (Roberts et al. 2020, Priestley and Catto 2022).

Recent advancements in climate modeling, such as the High Resolution Model Intercomparison Project (HighResMIP) under the Coupled Model Intercomparison Project Phase 6 (CMIP6) (Haarsma et al. 2016), have enabled the development of global climate models with atmospheric resolutions as fine as 25 km. These high-resolution models show promise in better representing extratropical cyclones and their associated processes compared to lower-resolution models. Studies have demonstrated improvements in simulating cyclone frequency, intensity, and structure, particularly in the Northern Hemisphere (Jung et al. 2006, Willison et al. 2013, Seiler et al. 2018, Li et al. 2021). For example, Priestley and Catto (2022) found that HighResMIP models reduce biases in extratropical cyclone-associated precipitation and winds, while Roberts et al. (2020) highlighted similar benefits for tropical cyclones. However, challenges persist in simulating the most intense systems, especially in the Southern Hemisphere, where biases in storm track location and intensity remain (Chang et al. 2012, Priestley et al. 2020).

While HighResMIP simulations have been extensively used to study Northern Hemisphere cyclones (Roberts et al. 2020, Tang et al. 2022, Priestley and Catto 2022), less attention has been given to the Southern Hemisphere, particularly to intense cyclones in regions such as southeast South America — a known hotspot for cyclogenesis where systems often exhibit rapid intensification and extreme characteristics (Lim and Simmonds 2002, Heidari et al. 2020, Andrade et al. 2024). Coarse resolution models tend to underestimate the frequency and intensity of these cyclones, especially for extreme events (Zappa et al. 2013, Seiler and Zwiers 2016), raising critical questions about the role of horizontal resolution in improving their representation. Although regional climate models offer refined resolution, high-resolution global models now provide a direct means to investigate these processes without downscaling (Willison et al. 2013, Seiler et al. 2018). The HighResMIP protocol, which facilitates direct comparisons between high- and low-resolution configurations with minimal additional tuning, offers a unique opportunity to isolate the effects of resolution on cyclone characteristics (Haarsma et al. 2016).

This study assesses how well HighResMIP models capture extratropical cyclones characteristics compared to standard CMIP6 models, focusing on the South Atlantic and southeastern South America cyclogenesis region. Specifically, we aim to:

- Identify improvements in the HighResMIP ensemble relative to standard (lower resolution) CMIP6 models.
- Examine whether increased resolution enhances the simulation of storm track frequency, intensity, and associated extreme events.

The paper is organized as follows: Section 2 describes the data, models, and methods used for tracking and analysing extratropical cyclones. Section 3 presents the results, focusing on differences between high- and low-resolution models. Finally, Section 4 discusses the findings, their implications, and directions for future research.

## 2 Data and methods

### 2.1 Reanalysis and model simulations

This study uses outputs from seven CMIP6 historical simulations (Eyring et al. 2016), categorized into high-resolution (25–50 km grid spacing) and low-resolution (100–250 km) groups. The high-resolution simulations are obtained from the Horizon2020 PRIMAVERA project (<https://www.primavera-h2020.eu>, accessed December 5, 2024), follow the High Resolution Model Intercomparison Project (HighResMIP, Haarsma et al. 2016) protocol and are fully coupled with identical forcings to the low-resolution historical experiment. All modeling centers provide at least two different resolutions for the atmospheric component, allowing directly assessment of the impact of model resolution. Key model variables include zonal (u) and meridional (v) wind at 850 hPa at 6-hourly resolution. Some models also provide additional variables such as mean sea level pressure (MSLP) and total precipitation for the same temporal frequency. Data is available from 1950, but the evaluation focuses on 1979–2014 to match the reanalysis. Further model details are provided in Table 1.

**Table 1** List of CMIP6 models used in this study. Atmospheric horizontal resolutions are provided as grid dimensions on a Gaussian latitude  $\times$  longitude grid, followed by their spectral truncation (if applicable) and the corresponding nominal resolution in kilometers.

Model name	Institution	Atmospheric horizontal resolution	
		Lat $\times$ Lon	Nominal
CMCC-CM2	Centro Euro-Mediterraneo per i Cambiamenti Climatici (CMCC, Italy)	288 $\times$ 192 ( $\sim 0.7^\circ$ )	100 km
		1152 $\times$ 768 ( $\sim 0.175^\circ$ )	25 km
CNRM-CM6-1	Centre Européen de Recherche et de Formation Avancée en Calcul Scientifique (CERFACS, France)	256 $\times$ 128 (T127)	250 km
		720 $\times$ 360 (T359)	50 km
FGOALS-f3	State Key Laboratory of Numerical Modeling for Atmospheric Sciences and Geophysical Fluid Dynamics (LASG, China)	320 $\times$ 180 (C96)	100 km
		1440 $\times$ 720 (C384)	25 km
ECMWF-IFS	European Centre for Medium Range Weather Forecasts (ECMWF, Europe)	360 $\times$ 181 (Tco199)	50 km
		360 $\times$ 181 (Tco199)	50 km
		720 $\times$ 361 (Tco399)	25 km
EC-Earth3P	EC-Earth Consortium (European research institutions)	512 $\times$ 256 (T255)	100 km
		1024 $\times$ 512 (T511)	50 km
HadGEM3-GC31	Met Office Hadley Centre (United Kingdom)	192 $\times$ 145 (N96)	250 km
		432 $\times$ 325 (N216)	100 km
		1024 $\times$ 769 (N512)	50 km
MPI-ESM1-2	Max Planck Institute for Meteorology (MPI-M, Germany)	192 $\times$ 196 (T63)	250 km
		768 $\times$ 384 (T255)	50 km

The model results are evaluated against ERA5, the latest global reanalysis from the European Centre for Medium-Range Weather Forecasts (ECMWF; Hersbach et al. 2020). ERA5 improves significantly over ERA-Interim by incorporating advanced model physics, refined dynamic core, and 4D-Var data assimilation system within the Integrated Forecast System (IFS) Cycle 41r2. With ~31 km resolution, hourly outputs, 137 vertical levels, and a broader range of assimilated observations, ERA5 offers a detailed and reliable atmospheric representation for assessing climate model performance.

## 2.2 Tracking and compositing

Cyclones are identified and tracked using the objective feature-tracking algorithm developed by Hodges (1994, 1995, 1999). In this study, we apply this method to compute the 850-hPa relative vorticity from 6-hourly wind data, spectrally truncated to T42 resolution, with planetary-scale wavenumbers ( $\leq 5$ ) removed. This retains synoptic-scale features and ensures a fair comparison across datasets with varying resolutions. Cyclones are identified as relative vorticity maxima exceeding  $1 \times 10^{-5} \text{ s}^{-1}$  (scaled by -1 for the Southern Hemisphere) and are refined using B-spline interpolation and steepest ascent maximization. Tracks are initialized by linking vorticity maxima using a nearest neighbor approach and further refined by minimizing a cost function for track smoothness, constrained by displacement distance. To focus on long-lived, mobile synoptic systems, only tracks with a minimum lifetime of 24 hours and a displacement distance of at least 1000 km are retained for analysis.

In this study, we focus on analyzing the characteristics of extratropical cyclones in the well-known genesis region over Uruguay (30°S, 60°W). A cyclone track is associated with this domain if at least 80% of its track points lie within the region. Spatial statistics are produced using spherical kernel estimators, as described by Hodges (1996). Track density is computed using a single point from each track closest to the estimation points, scaled to number per season per unit area, with the unit area equivalent to a 5° spherical cap (approximately  $10^6 \text{ km}^2$ ). Cyclone intensities are defined as the peak value of 850-hPa vorticity at T42 resolution across the cyclone life cycle. While analyses are performed for each season, only the mean fields are presented for simplicity.

The composite structure of cyclones is examined using a system-centered compositing approach, as described in Bengtsson et al. (2007, 2009) and Catto et al. (2010). For extreme cyclones, the 90th percentile of the most intense storms is used, defined by their maximum 850-hPa vorticity at T42. Atmospheric fields such as vorticity, horizontal winds, MSLP, and precipitation are sampled onto a 30° latitude-longitude grid with a 0.5° resolution, centered on the storm's vorticity center. The grid, initially aligned with the Equator, is not rotated to preserve geographical features. The composite fields represent the cyclones at their peak intensity to capture their most hazardous phase.

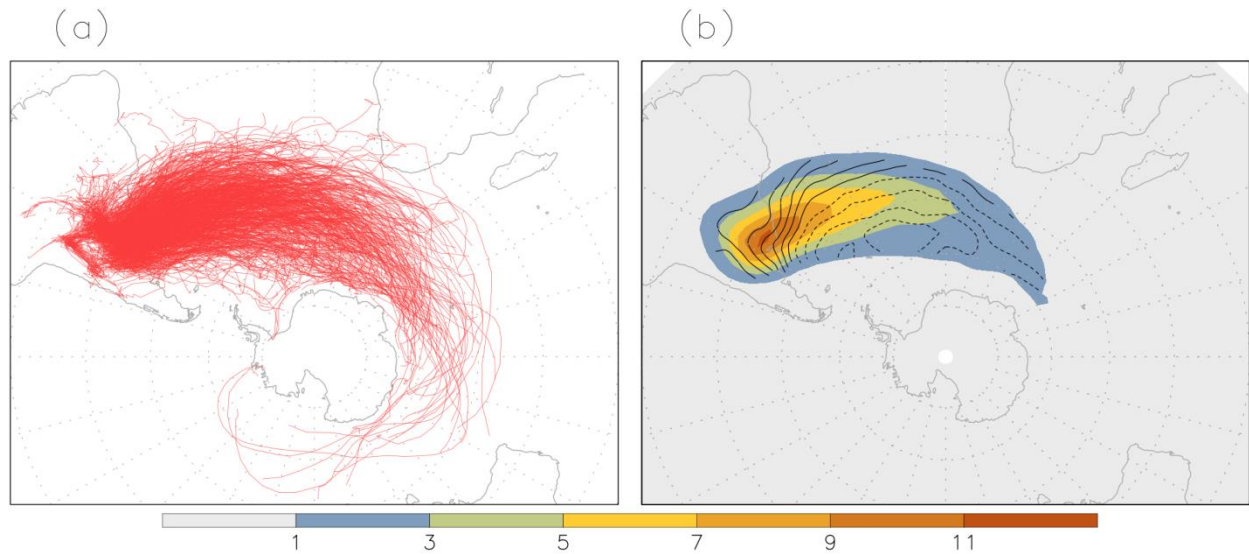
To examine the typical life cycle of extreme cyclones, single-value properties from full-resolution data are extracted along the storm tracks and centered on the time of maximum T42 850-hPa vorticity. Due to the asymmetrical structure of extratropical cyclones, key properties are derived using specific methods: pressure minima are identified by locally minimizing MSLP within a 5° radius of the storm center, while winds and vorticity are determined by finding the maximum values (or minimum for the Southern Hemisphere cyclonic vorticity) within the same radius. Precipitation is calculated as the area-averaged rate over the 5° radius. These properties are then averaged across specific stages of the cyclone's life cycle for further analysis.

## 125 3 Results

### 126 3.1 Cyclone spatial distribution

127 Because the focus of the study is on the low-level cyclonic systems originated in the La Plata River basin, it is of  
128 interest to first isolate those systems generated in this well-known genesis region and then analyze their statistics. This  
129 is done by applying an  $8^\circ$  radius spherical cap sampling centered on the cyclogenesis region over Uruguay ( $30^\circ\text{S}$ ,  
130  $60^\circ\text{W}$ ). Figure 1a provides an overview of all 1,406 tracks identified in ERA5 that originated in this region during the  
131 period 1979-2014, matching the period available for the models to ensure a consistent comparison. The main storm  
132 track spirals poleward from South America across the Atlantic and Indian Oceans and around Antarctica, with some  
133 long-lasting, mobile systems extending into the southern South Pacific.

134 To better understand the properties of these cyclones, statistical diagnostics computed from the feature track ensembles  
135 are produced. The corresponding track density and mean intensities are shown in Figure 1b. The 850-hPa vorticity track  
136 density averaged over all seasons captures the primary spiral storm track described above. As the cyclones moves  
137 downstream and poleward, their average intensities based on the T42 850-hPa vorticity increase, reaching values of  $6\text{--}8$   
138  $\times 10^{-5} \text{ s}^{-1}$  across the Atlantic and Indian Oceans. Notably, the track density and mean intensity closely resemble patterns  
139 observed in the older ERA-40 reanalysis for the same field (Hoskins and Hodges 2005, their Fig. 6), providing some  
140 confidence to their reproducibility.



141  
142 **Fig. 1** (a) Trajectories of all cyclones identified in the 850-hPa vorticity originating in the cyclogenesis region in the  
143 southeast South America. (b) Track density (shaded) and mean intensity (contour) for the same systems. Units represent  
144 the number per season per unit area ( $\cong 10^6 \text{ km}^2$ ) for track density and  $\text{s}^{-1}$  (scaled by  $-1 \times 10^{-5}$ ) for mean intensity for  
145 contour interval 0.5, ranging from 2.5 to 7.5. Statistics are produced using ERA5 data for the period 1979–2014.

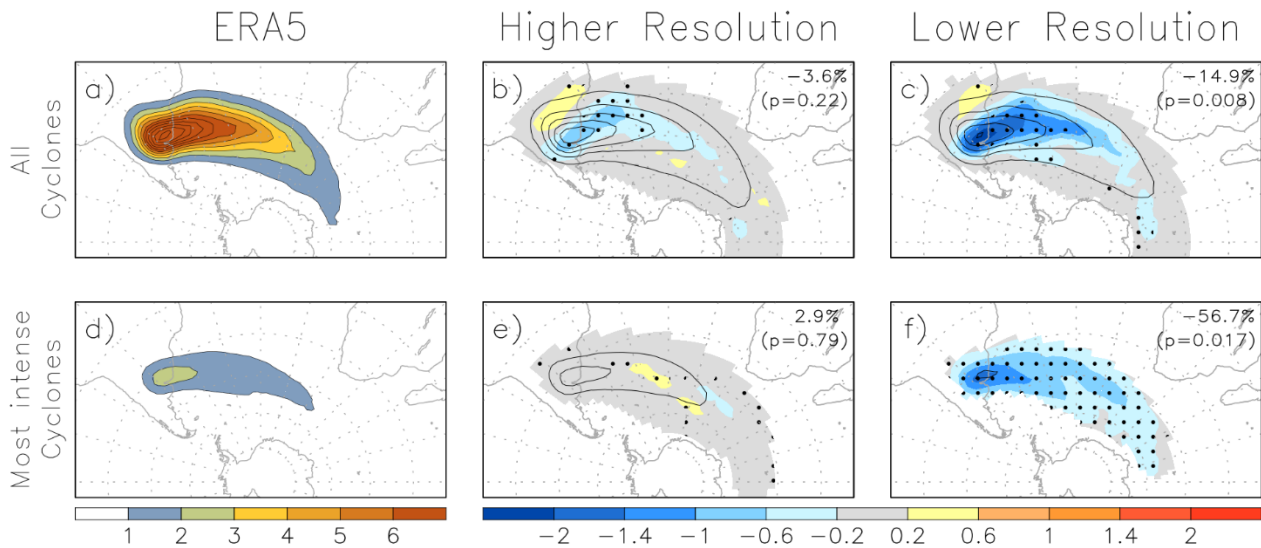
146 To assess the impact of model resolution on cyclone distribution, we compare the multi-model means of high- and low-  
147 resolution models to ERA5. Systematic biases are identified as regions where at least 80% of models exhibit the same  
148 bias signal. Figures 2b and 2c demonstrate that both multi-model means accurately capture the observed track density  
149 pattern (Figure 2a), but the high-resolution models exhibit lower bias. However, a notable equatorward shift in the



150 maximum track density is evident in both ensemble models, leading to underestimations over the key cyclogenesis  
 151 region. The pronounced equatorward bias in the track density has been attributed to biases in sea surface temperatures  
 152 and an underrepresentation of atmospheric temperature gradients across multiple generations of climate models (e.g.,  
 153 Trenberth and Fasullo 2010, Sallée et al. 2013, Priestley et al. 2020). Quantitatively, high-resolution models  
 154 underestimate cyclone track density by 3.6% ( $p=0.22$ ) and track number by 4.7%, while low-resolution models show  
 155 larger underestimations of 14.9% ( $p=0.008$ ) and 14.3%, respectively.

156 Figure 2e and 2f shows that the effect of model resolution is even more pronounced for the most intense cyclones,  
 157 defined as those with maximum T42 850-hPa vorticity exceeding the 90th percentile. Low-resolution models  
 158 significantly underestimate the frequency of these events, with a 56.7% ( $p=0.017$ ) reduction in track density and a  
 159 57.8% reduction in track number, with nearly all models displaying a negative bias. In contrast, high-resolution models  
 160 perform significantly better, with average differences of +2.9% ( $p=0.79$ ) and +2.6% for track density and number,  
 161 respectively. These findings highlight the importance of high-resolution models for accurately simulating extreme  
 162 events.

163



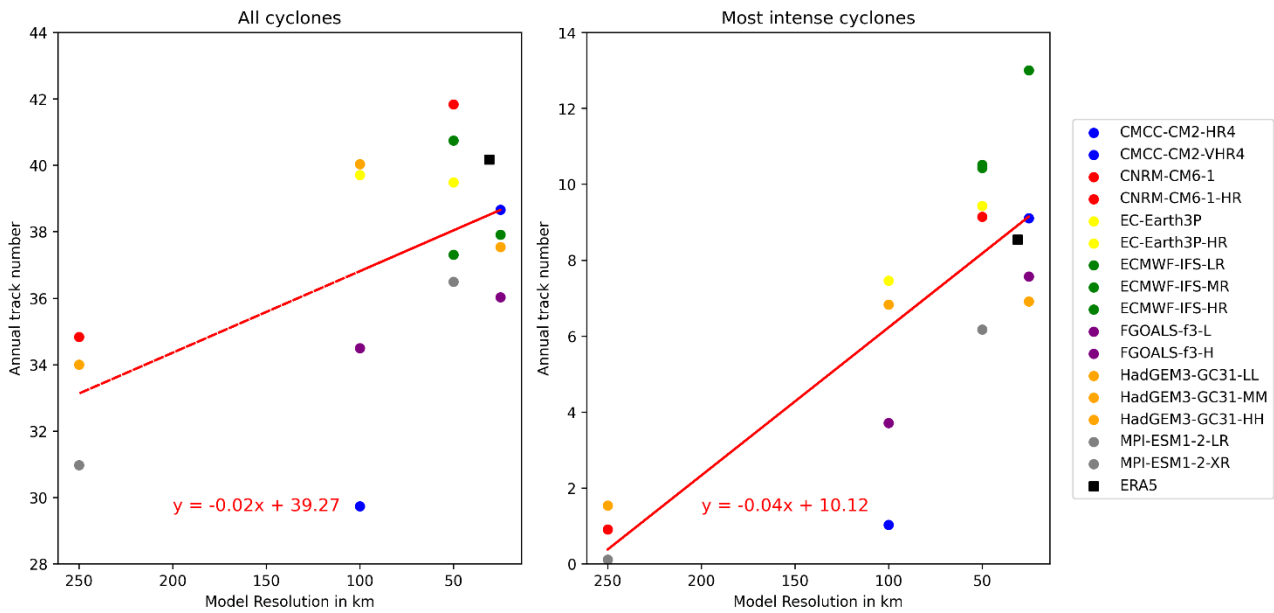
164

165 **Fig. 2** Cyclone track density based on 850-hPa relative vorticity for (a, d) ERA5 and for multi-model means of (b, e)  
 166 higher resolution models and (c, f) lower resolution models. The analysis includes (a, b, c) all cyclones and (d, e, f) the  
 167 most intense cyclones (90th percentile) based on the maximum T42 850-hPa relative vorticity. Biases are calculated  
 168 relative to ERA5 (multi-model mean minus reanalysis). Dotted areas represent regions where at least 80% of the models  
 169 agree on the signal. The numbers in panels (b, c, e, f) indicate the percentage change in the track density, with p-values  
 170 in parentheses.

### 171 3.2 Number

172 To quantitatively assess the sensitivity of cyclone frequency to model spatial resolution, Figure 3 presents scatter plots  
 173 of the annual number of cyclones identified in the cyclogenesis region of South America, including results from models  
 174 with up to three different horizontal resolutions. For the total number of cyclones, most models demonstrate an increase  
 175 in cyclone frequency with higher spatial resolution, with an average increase of 12% when the resolution is refined from

176 160 km to 40 km. On average, 34.4 cyclones per year are identified in the lower resolution models, increasing to 38.3 in  
 177 higher resolution models — closer to the observed annual average of 40.2 cyclones in reanalysis. The linear regression  
 178 line, shown in red, highlights a stronger relationship between cyclone frequency and spatial resolution for intense  
 179 cyclones. Specifically, the number of intense cyclones rises by approximately 250% in the higher resolution models  
 180 compared to lower resolution counterparts, with annual averages increasing from 3.6 in coarser resolution simulations  
 181 to 8.8 in finer resolution simulations — closely matching the observed value of 8.6 from reanalysis. This steep increase  
 182 underscores a pronounced dependency of intense cyclone detection on finer spatial resolution, indicating that high-  
 183 resolution models are essential for accurately capturing the most intense systems.



184  
 185 **Fig. 3** Scatter plots of the annual number of cyclones identified in the cyclogenesis region in the southeast South  
 186 America for (a) all cyclones and (b) the most intense cyclones (90th percentile), in relation to the model spatial  
 187 resolution. Linear regression lines and equations are shown in red.

### 188 3.3 Intensity

189 We now investigate whether higher resolution models more accurately represent the peak intensity of cyclones, as  
 190 measured by the maximum 850-hPa vorticity (scaled by -1) at full resolution. Figure 4 shows a skewed distribution  
 191 toward lower values in the reanalysis (black line), indicating that most cyclones are relatively weak, with fewer intense  
 192 systems. High-resolution models (blue line) closely reproduce this distribution, with a 99% correlation with ERA5,  
 193 while low-resolution models (red line) exhibit a broader peak skewed toward lower values and a slightly lower  
 194 correlation of 95%. The differences become more pronounced when focusing on the extremes of the distribution,  
 195 corresponding to the 90th percentile. For systems with intensities exceeding  $20 \times 10^{-5} \text{ s}^{-1}$  (inset plot), low-resolution  
 196 models underestimate their frequency by approximately 33%, whereas high-resolution models align more closely with  
 197 reanalysis. These results highlight the sensitivity of cyclone maximum intensity representation to spatial resolution,  
 198 with higher resolution simulations providing significantly improved performance. Notably, the ERA5 reanalysis has a  
 199 higher horizontal resolution than even the most advanced HighResMIP models, emphasizing the importance of finer  
 200 resolutions for capturing the most intense systems.

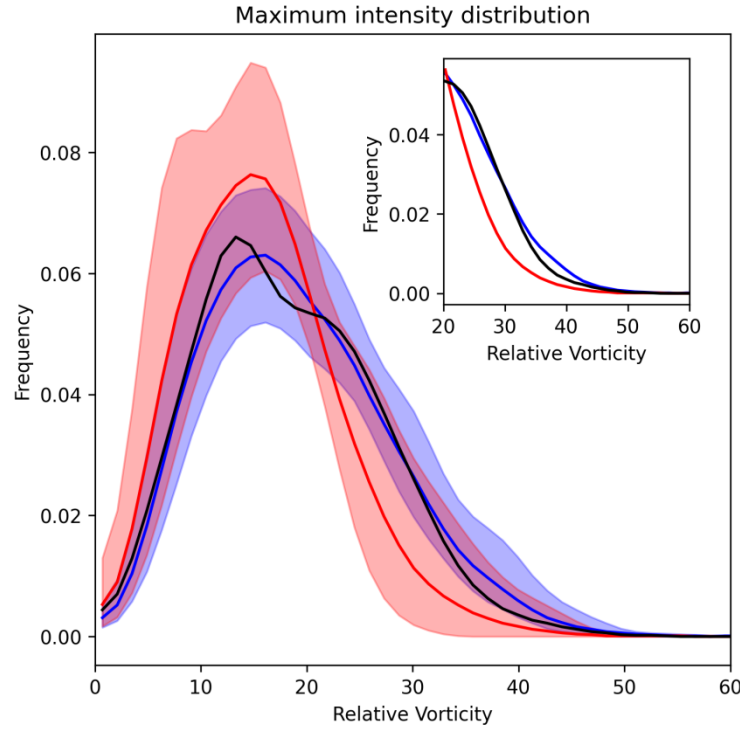


**Fig. 4** Maximum intensity distribution based on the 850-hPa relative vorticity at full resolution for cyclones identified in the ERA5 reanalysis (black line) and the multi-model ensembles of high-resolution (blue) and low-resolution (red) models. Shaded areas indicate the inter-model spread for each resolution group. The inset highlights the distribution of the most intense systems, corresponding to the 90th percentile. Unit is  $\text{s}^{-1}$ , scaled by  $-1 \times 10^{-5}$ .

### 3.4 Structure and lifecycle

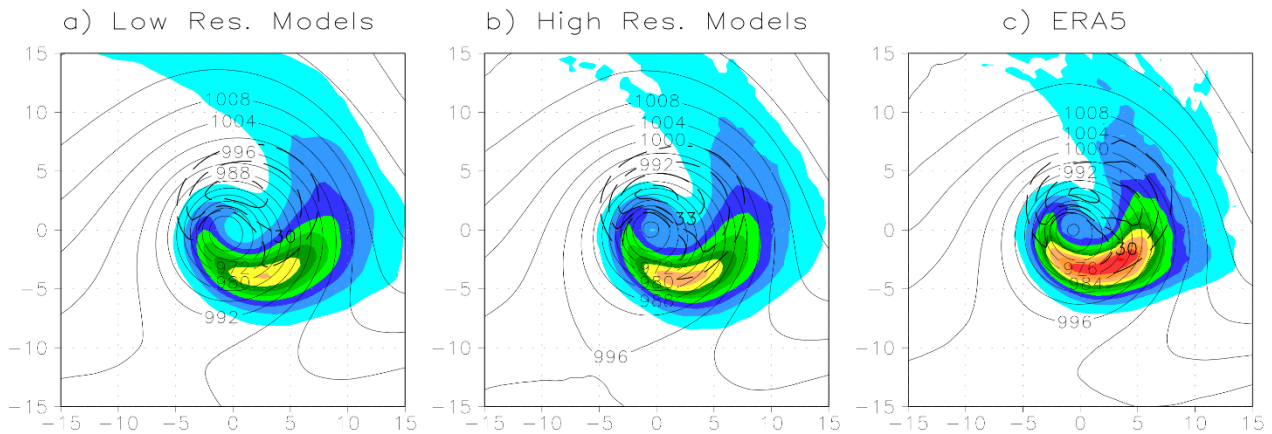
This section analyses the key synoptic features of extratropical cyclones by comparing the ensemble mean of both high- and low-resolution models to ERA5 reanalysis. Focusing on intense cyclones, a centered composite method is applied to the 90th percentile of the most intense cyclones in each model and reanalysis. Unlike previous studies (e.g., Bengtsson et al. 2009, Catto et al. 2010), the grid is not rotated based on the storm propagation direction, allowing features to be assessed within a geographically fixed framework.

Figure 5 presents the composite structure of the 90th percentile most intense cyclones, centered on the time and location of maximum intensity in the T42 relative vorticity at 850 hPa. The filtered vorticity, used for identification and tracking, is less noisy than the full-resolution vorticity and closely corresponds to the minimum MSLP during the storm's life cycle. At peak intensity, the MSLP exhibits an elongated southwest-northeast orientation with a deep low-pressure center co-located with the cyclone core. The minimum MSLP in ERA5 is 964 hPa, while both model ensembles show slightly lower values. Overall, the spatial patterns of the MSLP from both ensemble models compare well against ERA5, including the strong pressure gradients. However, the compositing process tends to smooth out the sharp frontal structures typically observed in synoptic charts.

A critical aspect of cyclone representation in climate models is the accurate simulation of precipitation, given its significant socio-economic impacts. Identifying systematic biases is therefore essential for ensuring the reliability of precipitation projections in extratropical cyclones. ERA5 composite reveals a distinct comma-shaped rainband, with

precipitation cyclonically wrapping around the cyclone center. Maximum precipitation rates (reaching up to 10 mm per 6h) are located east and poleward of the storm center, near the typical position of a warm front. While both model ensembles capture this characteristic precipitation pattern, the peak values are underestimated, especially in the lower resolution models. The largest biases occur in the ascent region, consistent with previous findings (e.g., Naud et al. 2020), suggesting that precipitation biases may be related to deficiencies in simulating vertical velocities. Furthermore, these could be linked to inaccuracies in representing large-scale dynamics and physical processes, such as latent heat release, which are key drivers of precipitation.

The 850-hPa wind speed in ERA5 displays an axially asymmetric distribution, with the strongest values equatorward of the storm center. These maximum winds are observed behind the approximate position of the cold front, along the comma tail of the rainband — a region typically characterized by dry conditions (Catto et al. 2010, Sinclair et al. 2020). Both ensemble models effectively capture the spatial wind patterns seen in ERA5, although wind speeds are underestimated in the lower resolution models. The strongest 850-hPa winds exceed  $36 \text{ m s}^{-1}$  in ERA5 and the higher resolution models, but are weaker in the lower resolution simulations. The differences in wind speed magnitude between resolutions suggest that model resolution plays a key role in representing extreme winds.



**Fig. 5** Composite cyclone of the 90th percentile most intense systems at the time of maximum vorticity for (a) low-resolution models, (b) high-resolution models, and (c) ERA5 reanalysis. The mean fields include mean sea level pressure (MSLP, solid contours, hPa), total precipitation (shading,  $\text{kg m}^{-2} \text{ s}^{-1}$ ), and 850-hPa wind speed (dashed contours,  $\text{m s}^{-1}$ ). Contour intervals are 4 hPa for MSLP and  $3 \text{ m s}^{-1}$  for wind speed.

We have previously demonstrated that the CMIP6 models can reproduce the spatial structure of extratropical cyclones, although certain properties are underrepresented, particularly in the lower resolution simulations. To further examine the influence of model resolution, we now evaluate their ability to simulate the temporal evolution of the same variables shown in Figure 5. For the life cycle compositing, each cyclone is centered at the time of its maximum intensity in the T42 relative vorticity at 850 hPa, as shown in Figure 6. Full-resolution data are used to determine the maximum relative vorticity, maximum winds, and minimum MSLP, which are identified within a  $5^\circ$  radius of the cyclone center at each time step throughout its lifetime. Precipitation is computed as the average within the same  $5^\circ$  radius of the cyclone center.

250 The results reveal substantial differences in the composite life cycle of maximum vorticity. Lower resolution models  
 251 significantly underestimate the peak values, whereas higher resolution models show better agreement with ERA5.  
 252 Nevertheless, even the higher resolution simulations exhibit a weaker peak intensity and slower strengthening rate  
 253 compared to reanalysis, although they reasonably capture the decay rate. These discrepancies, particularly during the  
 254 development stage, may be related to deficiencies in representing latent heat release, which plays a critical role in  
 255 generating eddy available potential energy and its subsequent conversion to eddy kinetic energy (Orlanski and Katzfey  
 256 1991).

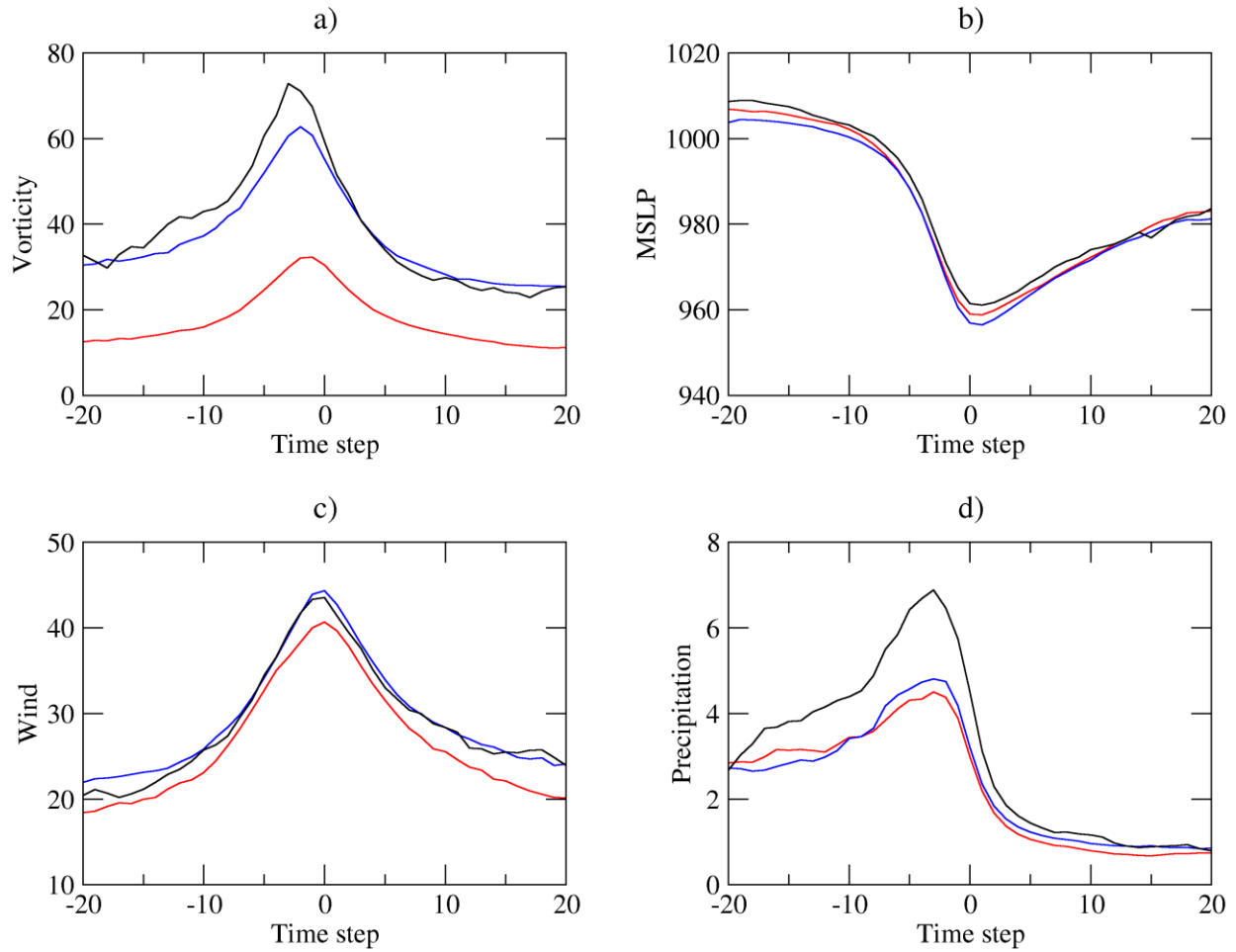
257 Quantitatively, the mean maximum vorticity for the most intense cyclones is  $72.8 \times 10^{-5} \text{ s}^{-1}$  in ERA5, compared to  $62.8$   
 258  $\times 10^{-5} \text{ s}^{-1}$  and  $32.3 \times 10^{-5} \text{ s}^{-1}$  in the high- and low-resolution models, respectively. Furthermore, the peak vorticities in  
 259 the full-resolution data occur earlier than the maxima identified in the T42 filtered vorticity, a behavior consistently  
 260 observed in both reanalysis and models. This lag time aligns with findings from previous studies on extratropical  
 261 cyclones (e.g., Bengtsson et al. 2009) and is likely attributed to the geostrophic adjustment process, during which the  
 262 wind (vorticity) field adjusts more rapidly than the mass (pressure) field (Temperton 1973).

263 The differences in the MSLP life cycle are relatively small. Model simulations produce slightly deeper systems  
 264 compared to ERA5, but the rates of deepening (as measured by MSLP) are nearly identical between the reanalysis and  
 265 models. Both reach a maximum deepening rate of approximately  $24 \text{ hPa h}^{-1}$  for 24h, clearly classifying these storms as  
 266 “bomb cyclones” (Sanders and Gyakum 1980). The better agreement between reanalysis and models for MSLP  
 267 compared to vorticity is likely due to the smoother, larger-scale nature of pressure fields, which are less sensitive to  
 268 resolution and fine-scale processes. In contrast, vorticity depends on accurate representation of wind gradients, which  
 269 are often underrepresented in relatively low-resolution models (Hoskins and Valdes 1990, Bengtsson et al. 2006).  
 270 Additionally, MSLP is more strongly constrained by observational data in reanalysis, while vorticity is derived from  
 271 model-dependent wind fields, making it more susceptible to errors and inconsistencies.

272 The peak precipitation occurs 18h before the time of maximum vorticity in both reanalysis and multi-model ensembles,  
 273 followed by a rapid decrease, likely due to the cyclones moving poleward into climatologically drier regions. It is  
 274 apparent that the precipitation is underestimated by the models with both ensemble models struggling to represent the  
 275 peak value as well as the rate of precipitation growth and decay. In relative terms, the average precipitation over all  
 276 offset times is underestimated by 23.5% and 16.8% in the lower and higher resolution models, respectively. This  
 277 underestimation is likely due to the inability of coarser resolution models to capture small-scale processes such as  
 278 mesoscale banding, frontal intensification, or localized convection, which are key contributors to extreme precipitation  
 279 in cyclones (Stephens et al. 2010, O’Gorman 2015, Hawcroft et al. 2018). These processes often occur on scales smaller  
 280 than the grid size of the models, making challenging for them to reproduce not only the intensity of peak precipitation  
 281 but also the rapid changes in precipitation rates associated with cyclone evolution. While the study uses ERA5 as a  
 282 reference, it acknowledges that the reanalysis data has also inherent uncertainties, particularly in precipitation estimates,  
 283 which is not directly assimilated but rather predicted by a short-range forecast, potentially introducing biases.

284 We also assess the simulations in terms of cyclone-related maximum wind speed. The strengthening of winds is clearly  
 285 linked to the increase in vorticity, a feature that is well captured by higher resolution models but underestimated in  
 286 coarser simulations. Low-resolution models systematically produce weaker maximum winds compared to high-  
 287 resolution models and reanalysis data, primarily due to their lower horizontal resolution which limits their ability to  
 288 accurately represent the wind-pressure relationship (Moon et al. 2021). These findings align with previous studies

289 demonstrating increased skill in simulating strong winds in intense cyclones at higher resolutions (e.g., Roberts et al.  
 290 2020, Li et al. 2021). Nevertheless, differences in wind speed are less pronounced than those in vorticity, which is  
 291 inherently more sensitive to spatial resolution and small-scale dynamical features.



292  
 293 **Fig. 6** Life cycle composites of the 90th percentile most intense cyclones identified in the T42 relative vorticity at 850  
 294 hPa for low-resolution models (red contour), high-resolution models (blue contour), and ERA5 reanalysis (black  
 295 contour). The parameters shown are (a) maximum 850-hPa relative vorticity (scaled by  $-1.0 \times 10^{-5} \text{ s}^{-1}$ ), (b) minimum  
 296 mean sea level pressure (MSLP, hPa), (c) maximum 850-hPa wind speed ( $\text{m s}^{-1}$ ), and (d) area-average total precipitation  
 297 ( $\text{kg m}^{-2} \text{ s}^{-1}$ ). All parameters are calculated within a  $5^\circ$  radius from the cyclone center using full resolution data.

## 298 4 Discussion and conclusions

299 This study presented a multi-model assessment of South American cyclone simulations using state-of-the-art climate  
 300 models, comparing HighResMIP simulations (grid spacings of 25–50 km) with standard-resolution CMIP6 models  
 301 (typically coarser than 100 km). The advantages of high-resolution models in simulating extratropical cyclones were  
 302 explored and quantified, demonstrating that increased horizontal resolution significantly improves the representation of  
 303 cyclones, particularly the extreme events.

304 While both high- and low-resolution models capture the observed track density pattern, high-resolution models exhibit  
 305 markedly lower biases, underestimating track density by only 3.6% compared to 14.9% in low-resolution models. For

intense cyclones, high-resolution models show near-perfect agreement with reanalysis, whereas low-resolution models underestimate their frequency by more than 50%. High-resolution models also provide a more accurate representation of cyclone intensity, displaying an exceptionally strong correlation with reanalysis in the distribution of maximum 850-hPa vorticity, while low-resolution models notably underestimate the frequency of extreme events. These findings align with previous studies (e.g., Roberts et al. 2020, Li et al. 2021, Moon et al. 2021, Priestley and Catto 2022), which have similarly demonstrated the critical role of high-resolution models in accurately simulating extreme cyclones and their associated dynamics across various regions.

The structure and life cycle of intense cyclones are better represented in high-resolution models, particularly in terms of vorticity and wind speed. Low-resolution models significantly underestimate the peak vorticity and exhibit slower strengthening rates, while high-resolution models show closer agreement with reanalysis. Both ensemble models effectively capture the deepening rates of MSLP, with high-resolution models producing slightly deeper systems. However, precipitation remains a persistent challenge, as both high- and low-resolution models underestimate its intensity throughout the cyclone life cycle and struggle to reproduce the rapid changes in precipitation rates observed in reanalysis. These discrepancies are likely due to limitations in resolving small-scale processes essential for generating extreme precipitation events.

The improvements observed in HighResMIP models can be attributed to several factors. First, the enhanced representation of moist processes, such as latent heat release, likely plays a key role in the rapid deepening of cyclones. Previous studies (e.g., Hirata et al. 2019, Willison et al. 2013) have shown that latent heat release is essential for the development of intense cyclones, and our results suggest that high-resolution models better capture these extreme events. Second, improved ocean-atmosphere coupling in coupled models may contribute to more accurate simulations of storm tracks. Studies such as Yao et al. (2008), Woollings et al. (2010), and Small et al. (2019) have demonstrated that higher ocean resolution enhances storm track representation through improved air-sea interactions. The models used in this study feature ocean resolutions ranging from 8 to 100 km, potentially impacting atmospheric circulation in varying ways. However, quantitatively attributing these improvements to either atmospheric or oceanic components remains challenging, as both are interdependent (Winton et al. 2013, Sein et al. 2018).

Despite these advancements, several limitations persist. High-resolution models are not specifically optimized for their finer grid spacings and rely on the same parameterizations as their lower-resolution counterparts. While this experimental design is valuable for isolating the effects of increased horizontal resolution, it does not guarantee that high-resolution simulations are inherently more realistic. Model biases, particularly those related to precipitation, highlight the need for continued refinement in model physics and resolution-specific tuning to enhance the accuracy of climate simulations. These challenges underscore a persistent limitation in accurately representing precipitation, an issue also evident in reanalysis products, emphasizing the complexity of capturing small-scale processes critical to extreme weather events.

The present study highlights the value of HighResMIP datasets for investigating future cyclone projections. For example, how intense and explosive cyclones will evolve under global warming in South America and surrounding oceans remains an important open question, which we aim to address in a follow-up study using HighResMIP future scenario outputs. Given the relevance of changes in extreme events associated with extratropical cyclones, it is crucial to explore future projections and associated uncertainties using finer resolution models. The comparative analysis



presented here provides a robust framework for model evaluation and bias identification, laying the groundwork for further analysis of cyclone characteristics under warming conditions.

Looking ahead, the upcoming phase of the High Resolution Model Intercomparison Project (HighResMIP2) within CMIP7 presents a critical opportunity to deepen our understanding of the role of horizontal resolution in climate simulations. Advances in high-performance computing and modeling techniques will enable more detailed investigations into the drivers and impacts of variability and change in extratropical cyclones and their associated large-scale features. Additionally, the emergence of global cloud-resolving models, currently limited to shorter timescales, offers a unique opportunity to bridge these simulations with traditional CMIP models, with HighResMIP2 serving as a key link. Initiatives such as Destination Earth (DestinE, <https://destination-earth.eu/>) and EERIE (<https://eerie-project.eu/>), which aim to achieve ultra-high resolutions of 5 to 10 km, will further refine projections of storm track intensity and precipitation. Continued research is essential to clarify the implications of these projected changes for regional weather hazards and broader climate impacts, ensuring more reliable and actionable climate information for decision-makers.

## References

- Andrade HN, Quadro MFL, Nunes AB, Oliveira FS, Avila VD, Teixeira MS, Alves RDCM (2024) Explosive cyclones occurred between 2010 and 2020 in the South Atlantic under the perspective of two detection schemes. *An Acad Bras Cienc* 96(suppl 1):e20231051. <https://doi.org/10.1590/0001-3765202420231051>
- Bengtsson L, Hodges KI, Roeckner E (2006) Storm tracks and climate change. *J Clim* 19:3518–3543. <https://doi.org/10.1175/JCLI3815.1>
- Bengtsson L, Hodges KI, Esch M, Keenlyside N, Kornblueh L, Luo JJ, Yamagata T (2007) How may tropical cyclones change in a warmer climate? *Tellus A* 59:539–561. <https://doi.org/10.1111/j.1600-0870.2007.00251.x> SCIRP+2Wiley Online Library+2pure.mpg.de+2
- Bengtsson L, Hodges KI, Keenlyside N (2009) Will extratropical storms intensify in a warmer climate? *J Clim* 22:2276–2301. <https://doi.org/10.1175/2008JCLI2678.1> ui.adsabs.harvard.edu+1Agupubs+1
- Bitencourt DP, Manoel G, Acevedo OC, Fuentes MV, Muza MN, Rodrigues ML, Leal Quadro MF (2011) Relating winds along the Southern Brazilian coast to extratropical cyclones. *Meteorol Appl* 18:223–229. <https://doi.org/10.1002/met.232>
- Catto JL, Shaffrey LC, Hodges KI (2010) Can climate models capture the structure of extratropical cyclones? *J Clim* 23:1621–1635. <https://doi.org/10.1175/2009JCLI3318.1>
- Chang EK, Guo Y, Xia X (2012) CMIP5 multimodel ensemble projection of storm track change under global warming. *J Geophys Res Atmos* 117:D23118. <https://doi.org/10.1029/2012JD018578>
- Eyring V, Bony S, Meehl GA, Senior CA, Stevens B, Stouffer RJ, Taylor KE (2016) Overview of the Coupled Model Intercomparison Project Phase 6 (CMIP6) experimental design and organization. *Geosci Model Dev* 9:1937–1958. <https://doi.org/10.5194/gmd-9-1937-2016>
- Gobato R, Heidari A (2020) Cyclone bomb hits southern Brazil in 2020. *J Atmos Sci Res* 3:30–35.



379 Haarsma RJ, Roberts MJ, Vidale PL, Senior CA, Bellucci A, Bao Q, et al. (2016) High resolution model  
380 intercomparison project (HighResMIP v1.0) for CMIP6. *Geosci Model Dev* 9:4185–4208. [https://doi.org/10.5194/gmd-](https://doi.org/10.5194/gmd-9-4185-2016)  
381 9-4185-2016

382 Hawcroft M, Walsh E, Hodges K, Zappa G (2018) Significantly increased extreme precipitation expected in Europe and  
383 North America from extratropical cyclones. *Environ Res Lett* 13:124006. <https://doi.org/10.1088/1748-9326/aae6e2>

384 Heidari A, Gobato R, Mitra A, Gobato MRR (2020) Cotes's Spiral Vortex in Extratropical Cyclone Bomb South Atlantic  
385 Oceans. *Aswan Univ J Environ Stud* 1:147–156.

386 Hersbach H, Bell B, Berrisford P, Hirahara S, Horányi A, Muñoz-Sabater J, et al. (2020) The ERA5 global reanalysis. *Q*  
387 *J R Meteorol Soc* 146:1999–2049. <https://doi.org/10.1002/qj.3803>

388 Hirata H, Kawamura R, Nonaka M, Tsuboki K (2019) Significant impact of heat supply from the Gulf Stream on a  
389 “superbomb” cyclone in January 2018. *Geophys Res Lett* 46:7718–7725. <https://doi.org/10.1029/2019GL083546>

390 Hodges KI (1994) A general method for tracking analysis and its application to meteorological data. *Mon Weather Rev*  
391 122:2573–2586. [https://doi.org/10.1175/1520-0493\(1994\)122<2573:AGMFTA>2.0.CO;2](https://doi.org/10.1175/1520-0493(1994)122<2573:AGMFTA>2.0.CO;2)

392 Hodges KI (1995) Feature tracking on the unit sphere. *Mon Weather Rev* 123:3458–3465. [https://doi.org/10.1175/1520-](https://doi.org/10.1175/1520-0493(1995)123<3458:FTOTUS>2.0.CO;2)  
393 0493(1995)123<3458:FTOTUS>2.0.CO;2

394 Hodges KI (1996) Spherical nonparametric estimators applied to the UGAMP model integration for AMIP. *Mon*  
395 *Weather Rev* 124:2914–2932. [https://doi.org/10.1175/1520-0493\(1996\)124<2914:SNEATT>2.0.CO;2](https://doi.org/10.1175/1520-0493(1996)124<2914:SNEATT>2.0.CO;2)

396 Hodges KI (1999) Adaptive constraints for feature tracking. *Mon Weather Rev* 127:1362–1373.  
397 [https://doi.org/10.1175/1520-0493\(1999\)127<1362:ACFFT>2.0.CO;2](https://doi.org/10.1175/1520-0493(1999)127<1362:ACFFT>2.0.CO;2)

398 Hoskins BJ, Valdes PJ (1990) On the existence of storm-tracks. *J Atmos Sci* 47:1854–1864.  
399 [https://doi.org/10.1175/1520-0469\(1990\)047<1854:OTEOST>2.0.CO;2](https://doi.org/10.1175/1520-0469(1990)047<1854:OTEOST>2.0.CO;2)

400 Hoskins BJ, Hodges KI (2005) A new perspective on Southern Hemisphere storm tracks. *J Clim* 18:4108–4129.  
401 <https://doi.org/10.1175/JCLI3570.1>

402 Jung T, Gulev SK, Rudeva I, Soloviev V (2006) Sensitivity of extratropical cyclone characteristics to horizontal  
403 resolution in the ECMWF model. *Q J R Meteorol Soc* 132:1839–1857. <https://doi.org/10.1256/qj.05.212>

404 Li J, Bao Q, Liu Y, Wang L, Yang J, Wu G, et al. (2021) Effect of horizontal resolution on the simulation of tropical  
405 cyclones in the Chinese Academy of Sciences FGOALS-f3 climate system model. *Geosci Model Dev* 14:6113–6133.  
406 <https://doi.org/10.5194/gmd-14-6113-2021>

407 Lim EP, Simmonds I (2002) Explosive cyclone development in the Southern Hemisphere and a comparison with  
408 Northern Hemisphere events. *Mon Weather Rev* 130:2188–2209. [https://doi.org/10.1175/1520-](https://doi.org/10.1175/1520-0493(2002)130<2188:ECDITS>2.0.CO;2)  
409 0493(2002)130<2188:ECDITS>2.0.CO;2

410 Moon J, Park J, Cha DH (2021) Does increasing model resolution improve the real-time forecasts of western North  
411 Pacific tropical cyclones? *Atmosphere* 12:776. <https://doi.org/10.3390/atmos12060776>

412 Naud CM, Jeyaratnam J, Booth JF, Zhao M, Gettelman A (2020) Evaluation of modeled precipitation in oceanic  
413 extratropical cyclones using IMERG. *J Climate* 33(1):95–113

414 O’Gorman PA (2015) Precipitation extremes under climate change. *Curr Clim Change Rep* 1:49–59

415 Orlanski I, Katzfey J (1991) The life cycle of a cyclone wave in the Southern Hemisphere. Part I: Eddy energy budget. *J*  
416 *Atmos Sci* 48(17):1972–1998

417 Priestley MD, Ackerley D, Catto JL, Hodges KI, McDonald RE, Lee RW (2020) An overview of the extratropical storm  
418 tracks in CMIP6 historical simulations. *J Climate* 33(15):6315–6343

419 Priestley MD, Catto JL (2022) Improved representation of extratropical cyclone structure in HighResMIP models.  
420 *Geophys Res Lett* 49(5):e2021GL096708

421 Roberts MJ, Camp J, Seddon J, Vidale PL, Hodges K, Vanniere B, et al (2020) Impact of model resolution on tropical  
422 cyclone simulation using the HighResMIP–PRIMAVERA multimodel ensemble. *J Climate* 33(7):2557–2583

423 Sallée JB, Shuckburgh E, Bruneau N, Meijers AJ, Bracegirdle TJ, Wang Z, Roy T (2013) Assessment of Southern  
424 Ocean water mass circulation and characteristics in CMIP5 models: Historical bias and forcing response. *J Geophys Res*  
425 *Oceans* 118(4):1830–1844

426 Sanders F, Gyakum JR (1980) Synoptic-dynamic climatology of the “bomb”. *Mon Weather Rev* 108(10):1589–1606

427 Seiler C, Zwiers FW (2016) How well do CMIP5 climate models reproduce explosive cyclones in the extratropics of  
428 the Northern Hemisphere? *Clim Dyn* 46(3):1241–1256

429 Seiler C, Zwiers FW, Hodges KI, Scinocca JF (2018) How does dynamical downscaling affect model biases and future  
430 projections of explosive extratropical cyclones along North America’s Atlantic coast? *Clim Dyn* 50:677–692

431 Sein DV, Koldunov NV, Danilov S, Sidorenko D, Wekerle C, Cabos W, et al (2018) The relative influence of  
432 atmospheric and oceanic model resolution on the circulation of the North Atlantic Ocean in a coupled climate model. *J*  
433 *Adv Model Earth Syst* 10(8):2026–2041

434 Sinclair VA, Rantanen M, Haapanala P, Räisänen J, Järvinen H (2020) The characteristics and structure of extra-tropical  
435 cyclones in a warmer climate. *Weather Clim Dyn* 1:1–25

436 Small RJ, Msadek R, Kwon YO, Booth JF, Zarzycki C (2019) Atmosphere surface storm track response to resolved  
437 ocean mesoscale in two sets of global climate model experiments. *Clim Dyn* 52:2067–2089

438 Stephens GL, L’Ecuyer T, Forbes R, Gettelmen A, Golaz JC, Bodas-Salcedo A, et al (2010) Dreary state of precipitation  
439 in global models. *J Geophys Res Atmos* 115(D24)

440 Tang Y, Huangfu J, Huang R, Chen W (2022) Simulation and projection of tropical cyclone activities over the Western  
441 North Pacific by CMIP6 HighResMIP. *J Climate* 35(23):7771–7794

442 Temperton C (1973) Some experiments in dynamic initialization for a simple primitive equation model. *Q J R Meteorol*  
443 *Soc* 99(420):303–319

444 Trenberth KE, Fasullo JT (2010) Simulation of present-day and twenty-first-century energy budgets of the southern  
 445 oceans. *J Climate* 23(2):440–454

446 Willison J, Robinson WA, Lackmann GM (2013) The importance of resolving mesoscale latent heating in the North  
 447 Atlantic storm track. *J Atmos Sci* 70(7):2234–2250

448 Winton M, Adcroft A, Griffies SM, Hallberg RW, Horowitz LW, Stouffer RJ (2013) Influence of ocean and atmosphere  
 449 components on simulated climate sensitivities. *J Climate* 26(1):231–245

450 Woollings T, Hoskins B, Blackburn M, Hassell D, Hodges K (2010) Storm track sensitivity to sea surface temperature  
 451 resolution in a regional atmosphere model. *Clim Dyn* 35:341–353

452 Yao Y, Perrie W, Zhang W, Jiang J (2008) Characteristics of atmosphere-ocean interactions along North Atlantic  
 453 extratropical storm tracks. *J Geophys Res Atmos* 113(D14)

454 Zappa G, Shaffrey LC, Hodges KI (2013) The ability of CMIP5 models to simulate North Atlantic extratropical  
 455 cyclones. *J Climate* 26(15):5379–5396

456 **Statements & Declarations**

457 **Funding:** This research was supported by CNPq (151225/2023-0) and FAPESP (2023/10882-2).

458 **Competing Interests:** The authors have no relevant financial or non-financial interests to disclose.

459 **Author Contributions:** All authors contributed to the study conception and design. Material preparation, data  
 460 processing, and analysis were performed by Henri Pinheiro. The first draft of the manuscript was written by Henri  
 461 Pinheiro, and all authors provided feedback on earlier versions of the manuscript. All authors read and approved the  
 462 final manuscript.

463 **Data Availability:** The data used in this study are available from publicly accessible sources. CMIP6 model data were  
 464 obtained from the World Climate Research Programme’s Working Group on Coupled Modelling and can be accessed  
 465 via the Earth System Grid Federation (ESGF) at <https://esgf-index1.ceda.ac.uk/search/cmip6-ceda/>. ERA5 reanalysis  
 466 data were retrieved from the Copernicus Climate Change Service’s Climate Data Store at  
 467 <https://cds.climate.copernicus.eu/>, accessed on 25 March 2025.

Figure 1

[Click here to access/download;Figure;Fig1.png](#)

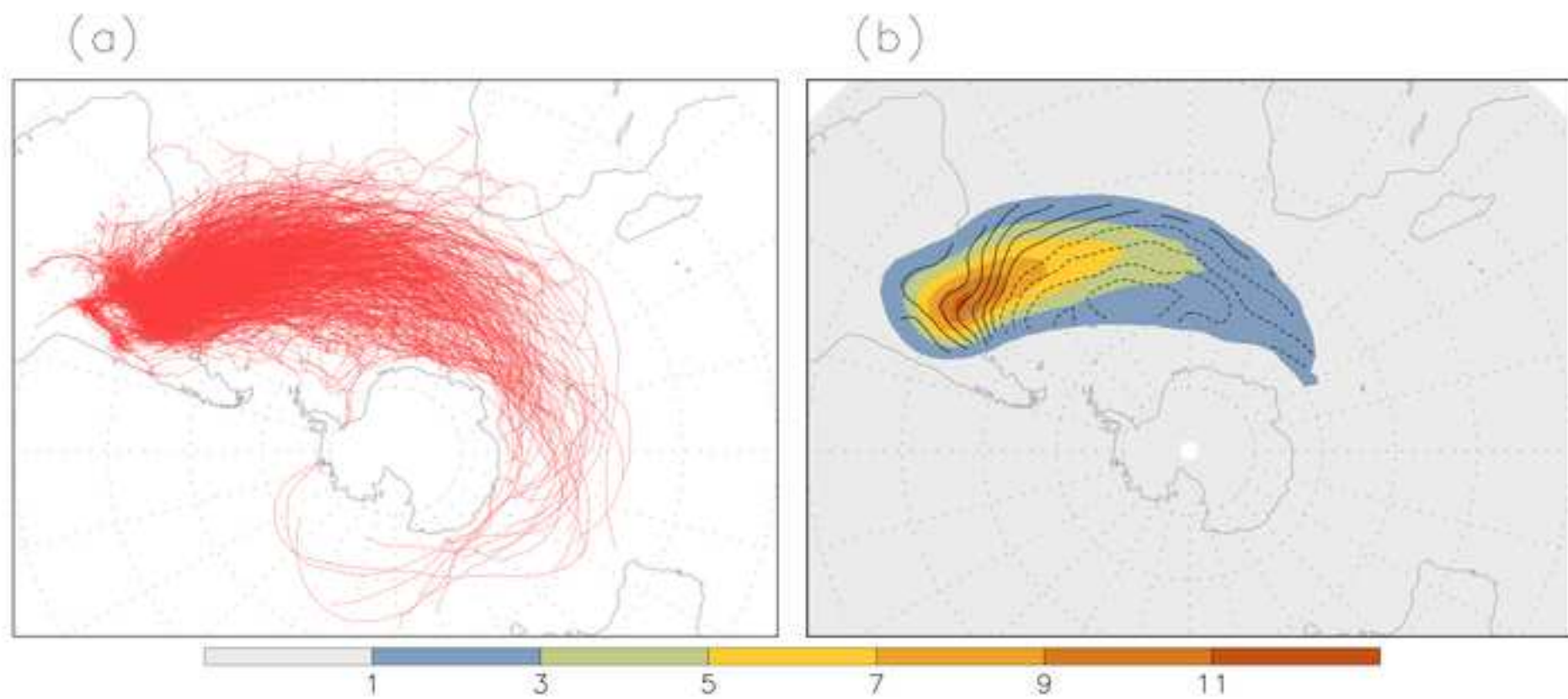


Figure 2

[Click here to access/download;Figure;Fig2.png](#)

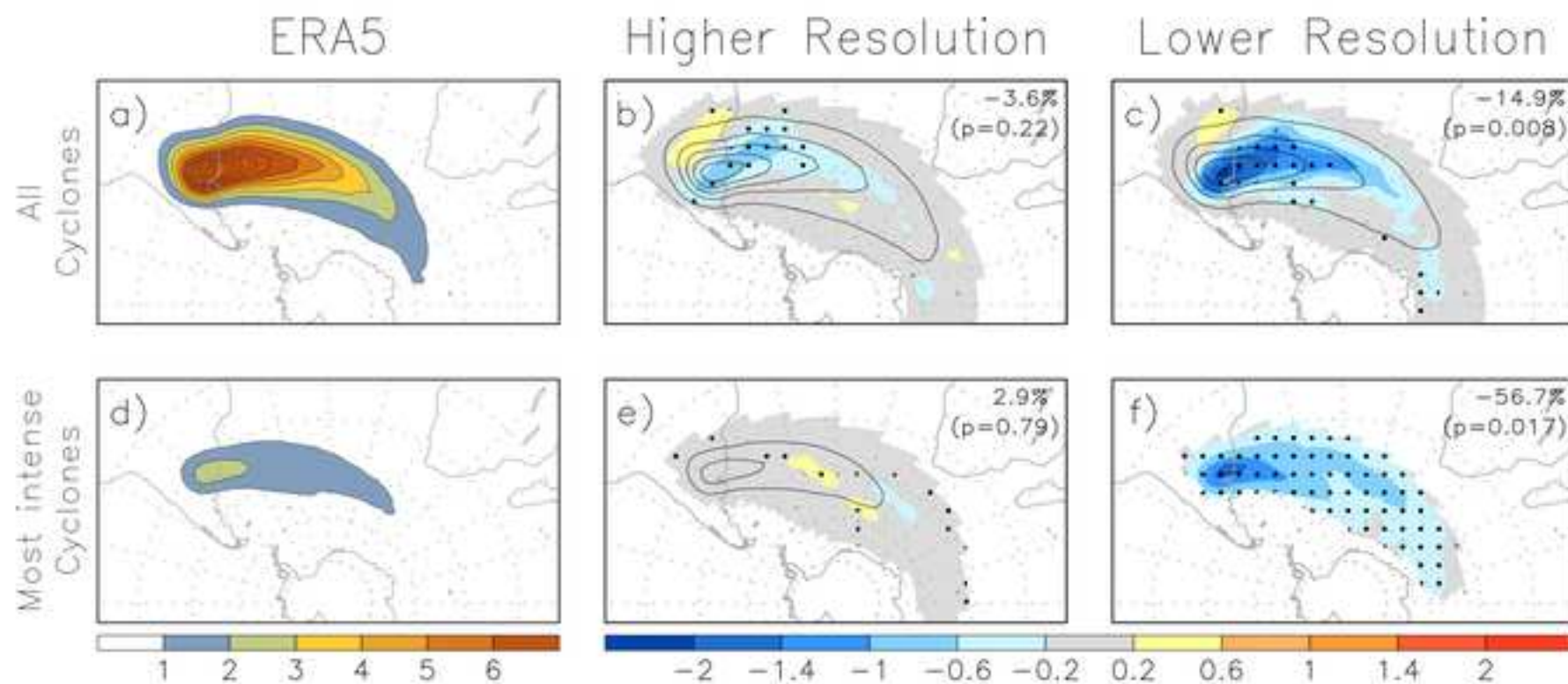


Figure 3

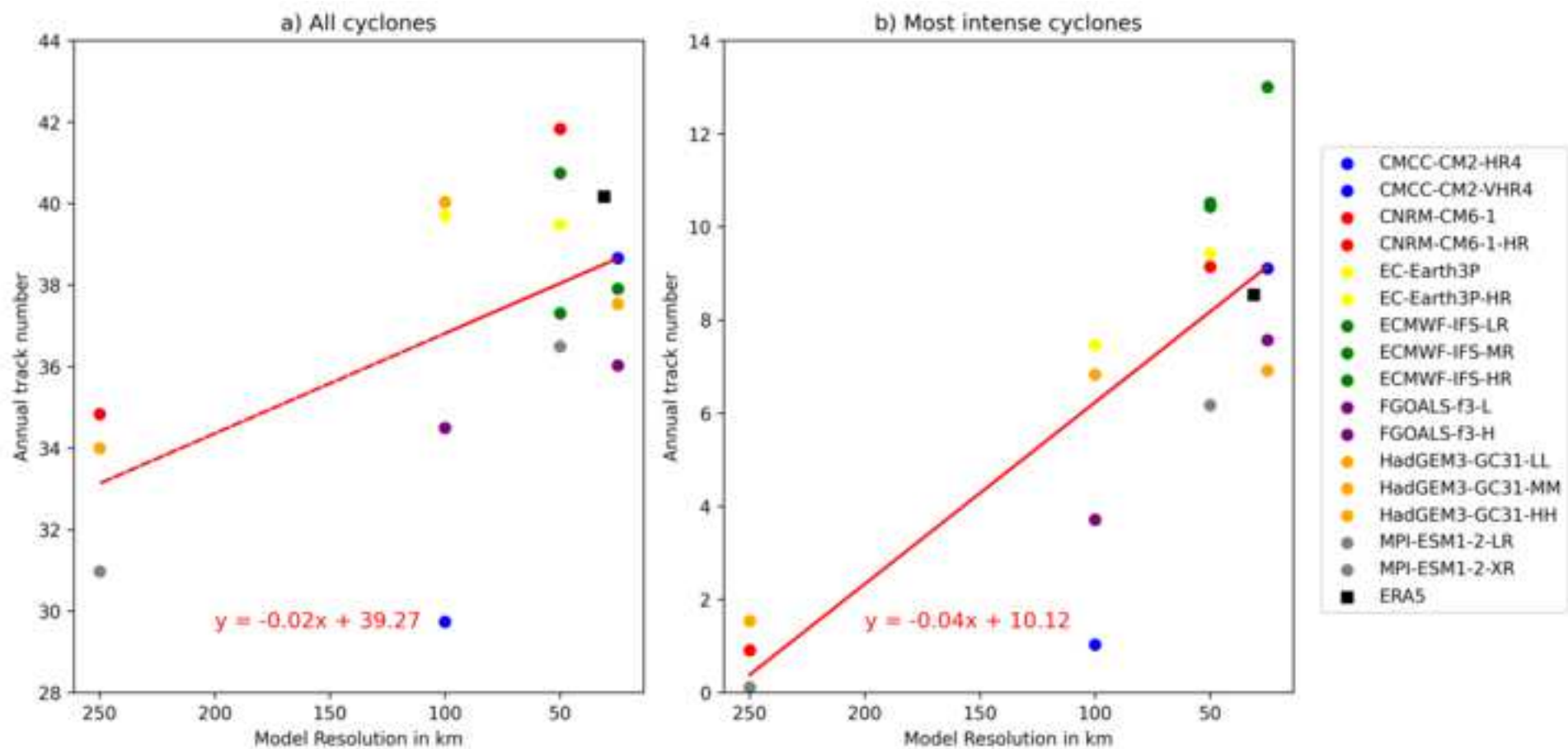


Figure 4

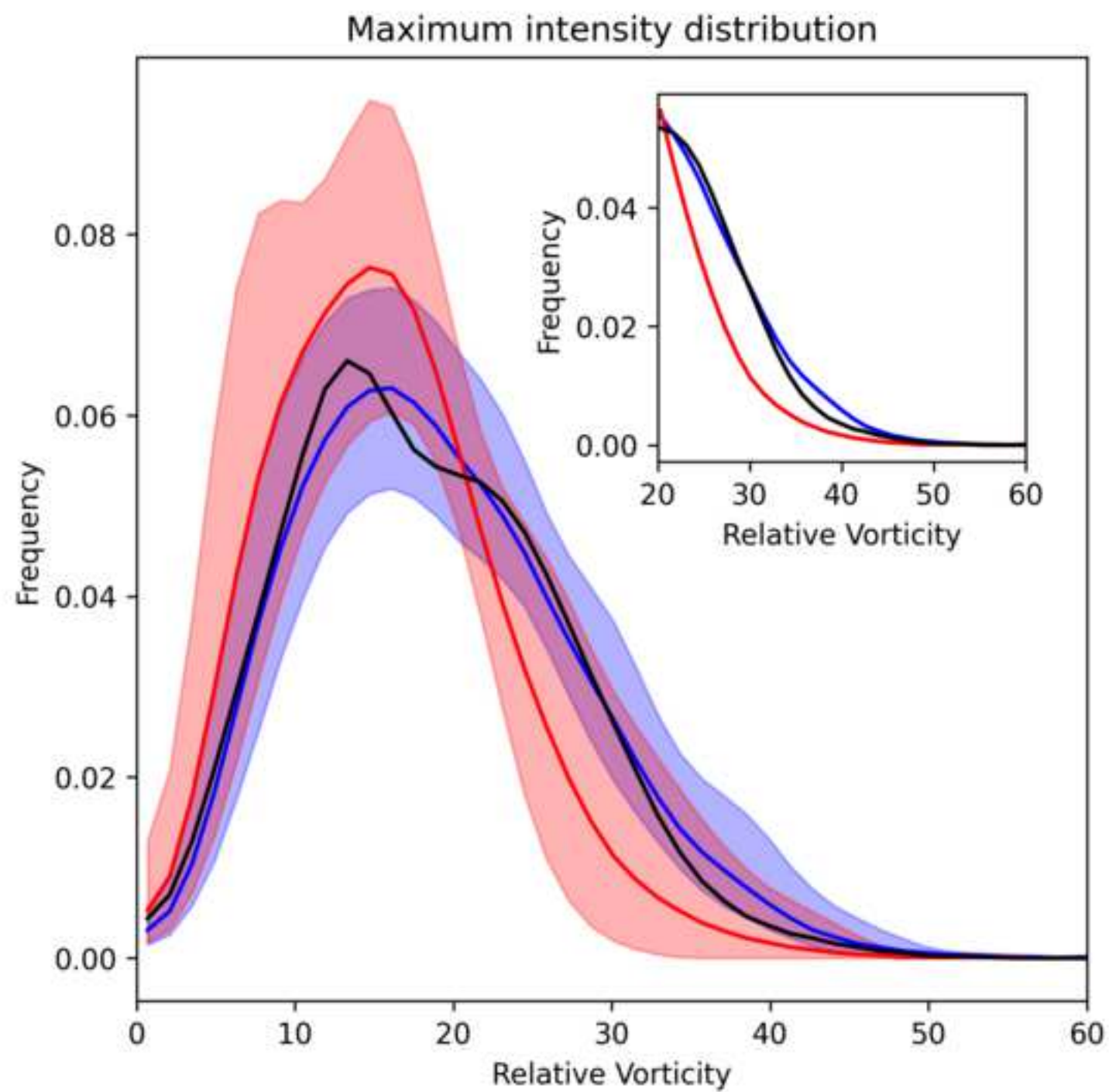




Figure 5

[Click here to access/download;Figure;Fig5.png](#)

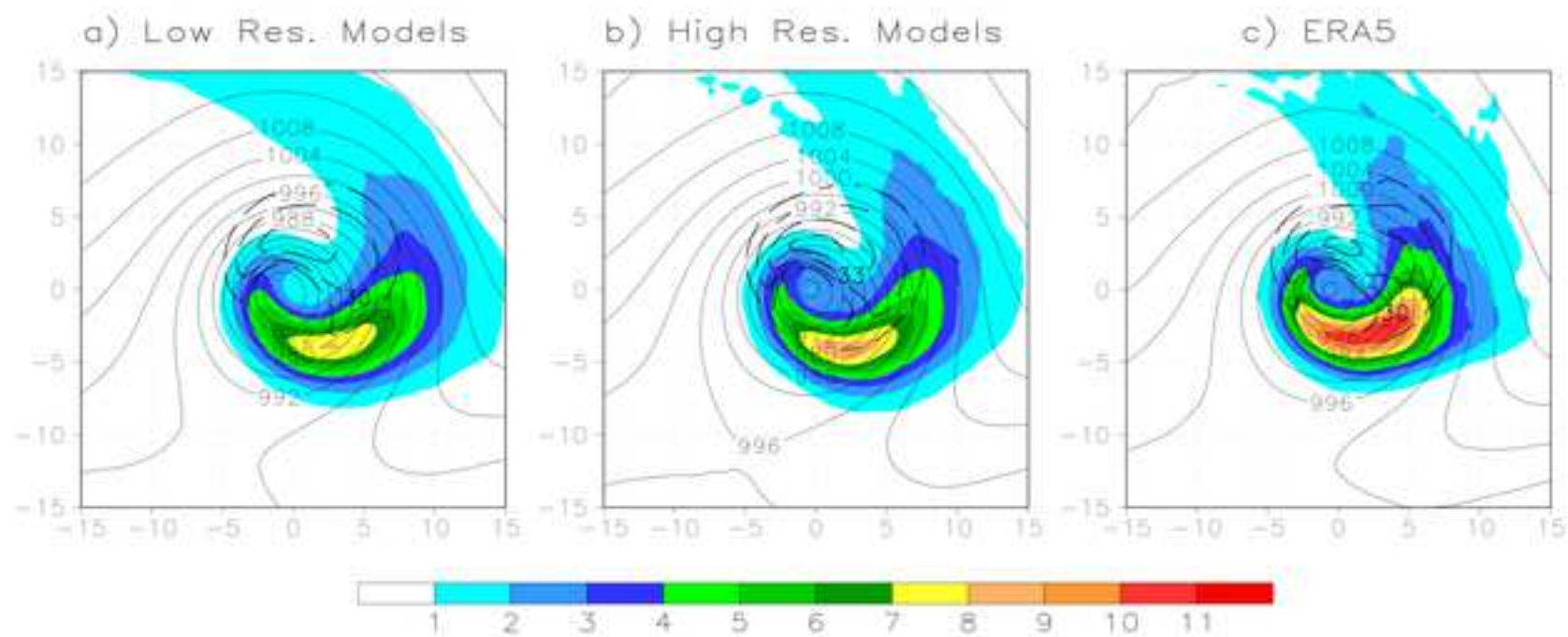
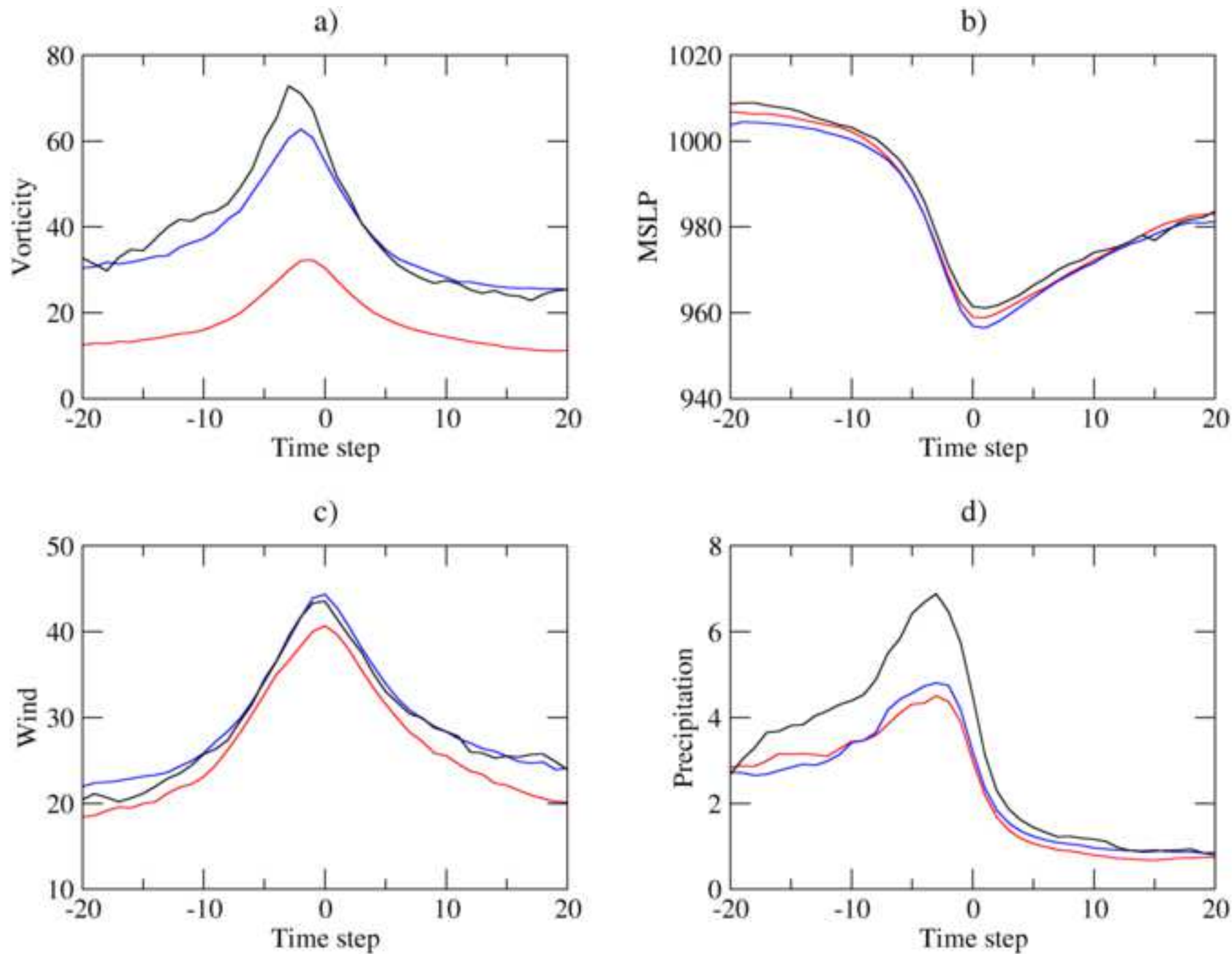




Figure 6



paper

Model name	Institution
CMCC-CM2	Centro Euro-Mediterraneo per i Cambiamenti Climatici (CMCC, Italy)
CNRM-CM6-1	Centre Européen de Recherche et de Formation Avancée em Calcul Scientifique (CERFACS, France)
FGOALS-f3	State Key Laboratory of Numerical Modeling for Atmospheric Sciences and Geophysical Fluid Dynamics (LASG, China)
ECMWF-IFS	European Centre for Medium Range Weather Forecasts (ECMWF, Europe)
EC-Earth3P	EC-Earth Consortium (European research institutions)
HadGEM3-GC31	Met Office Hadley Centre (United Kingdom)
MPI-ESM1-2	Max Planck Institute for Meteorology (MPI-M, Germany)

<b>Atmospheric horizontal resolution</b>	
<b>Lat × Lon</b>	<b>Nominal</b>
288 × 192 (~0.7°)	100 km
1152 × 768 (~0.175°)	25 km
256 × 128 (T127)	250 km
720 × 360 (T359)	50 km
320 × 180 (C96)	100 km
1440 × 720 (C384)	25 km
360 × 181 (Tco199)	50 km
360 × 181 (Tco199)	50 km
720 × 361 (Tco399)	25 km
512 × 256 (T255)	100 km
1024 × 512 (T511)	50 km
192 × 145 (N96)	250 km
432 × 325 (N216)	100 km
1024 × 769 (N512)	50 km
192 × 196 (T63)	250 km
768 × 384 (T255)	50 km